



# Cyanobacteria-Dominated Phytoplankton in the Oligotrophic South China Sea Maintain Photosynthetic Potential Despite Diurnal Photoinactivation of PSII

Xiangqi Yi<sup>1,2</sup>, Di Zhang<sup>2</sup>, Jiazhen Sun<sup>2</sup>, John Beardall<sup>3</sup> and Kunshan Gao<sup>2\*</sup>

<sup>1</sup> State Key Laboratory of Marine Environmental Science, College of the Environment and Ecology, Xiamen University, Xiamen, China, <sup>2</sup> State Key Laboratory of Marine Environmental Science, College of the Ocean and Earth Sciences, Xiamen University, Xiamen, China, <sup>3</sup> School of Biological Sciences, Monash University, Clayton, VIC, Australia

## OPEN ACCESS

### Edited by:

Punyasloke Bhadury,  
Indian Institute of Science Education  
and Research Kolkata, India

### Reviewed by:

Rajani Kanta Mishra,  
Ministry of Earth Sciences, India  
Sriyutha Murthy,  
Bhabha Atomic Research Center,  
India

### \*Correspondence:

Kunshan Gao  
ksgao@xmu.edu.cn

### Specialty section:

This article was submitted to  
Marine Biology,  
a section of the journal  
Frontiers in Marine Science

Received: 05 July 2021

Accepted: 30 September 2021

Published: 29 October 2021

### Citation:

Yi X, Zhang D, Sun J, Beardall J  
and Gao K (2021)  
Cyanobacteria-Dominated  
Phytoplankton in the Oligotrophic  
South China Sea Maintain  
Photosynthetic Potential Despite  
Diurnal Photoinactivation of PSII.  
Front. Mar. Sci. 8:736586.  
doi: 10.3389/fmars.2021.736586

In the warm, oligotrophic oceans, phytoplankton frequently experience high light exposure and must compete for a potentially limited nutrient supply. Additionally, the light regimes are dynamic in view of the diel solar cycle, weather conditions, and depth. Dealing with these challenges is critical to their survival. Here, we explored, using active chlorophyll *a* fluorescence, the photophysiological responses of cyanobacteria-dominated phytoplankton assemblages to intra-day variations in the light regime in the oligotrophic South China Sea (SCS). Experiments were conducted at three stations (SEATS, DC2, and DC6) where phytoplankton communities were dominated by *Prochlorococcus* and *Synechococcus*, and environmental conditions were similar except for daytime light conditions. We found that, at each station, the maximum quantum yield of PSII ( $F_v/F_m$ ) at dawn was as high as  $\sim 0.5$ , although concentrations of both dissolved inorganic nitrogen and soluble reactive phosphate were below the detection limits. Subsequently, diurnal patterns of  $F_v/F_m$  diverged between stations. At stations DC2 and DC6, we observed significant drops (25–48%) of  $F_v/F_m$  around midday, coinciding with the incident solar photosynthetically active radiation (PAR) reaching over  $2,000 \mu\text{mol quanta m}^{-2} \text{s}^{-1}$ , but  $F_v/F_m$  was nearly stable at SEATS where the daily maximal PAR was less than  $1,000 \mu\text{mol quanta m}^{-2} \text{s}^{-1}$ . Further analysis suggests that the midday drops in  $F_v/F_m$  at DC2 and DC6 were a consequence of high light-induced PSII photoinactivation. On the other hand, we found that the patterns of diurnal variation in maximum relative electron transport rate ( $rETR_{\text{max}}$ ) presented as being unimodal with a peak around midday at all three stations. Furthermore, we found that the diurnal pattern of  $rETR_{\text{max}}$  was mainly controlled by the extent of photochemical quenching (qP) which reflects the redox status of electron carriers downstream of PSII. In conclusion, our results indicate that, in the oligotrophic SCS, through increasing the activity of the electron-consuming mechanisms (high qP), the phytoplankton communities are able to maintain their midday photosynthetic potential (high  $rETR_{\text{max}}$ ) even with a degree of PSII photoinactivation (low  $F_v/F_m$ ).

**Keywords:** photoinactivation, active Chl *a* fluorescence, phytoplankton, South China Sea, diurnal variation

## INTRODUCTION

Marine phytoplankton are responsible for approximately half of global net primary production (Field et al., 1998; Westberry et al., 2008; Zhao and Running, 2010). This production supports nearly all life in the oceans and substantially affects global biogeochemical cycles and climate. The distribution and abundance of marine phytoplankton, being spatially and temporally dynamic, are mainly controlled by such key environmental drivers as temperature, nutrients, and light (Falkowski and Raven, 2007). Light is, on the one hand, the driving force of photosynthesis, but on the other hand, excessive light can inhibit photosynthesis and present a threat to phytoplankton (Raven, 2011; Campbell and Serôdio, 2020). In the oceans, the light regimes to which phytoplankton are exposed are primarily determined by solar irradiance, and thus present as periodically variable, with diel and seasonal cycles. Superimposed on such regularity are chaotic and stochastic variations relating to meteorological conditions such as cloud cover, precipitation, and atmospheric aerosol concentration and composition. Moreover, as solar irradiance enters the marine system, it is further absorbed and scattered by seawater, dissolved organic materials and particles, including photosynthetic organisms. Thus, the light regime for phytoplankton can be highly variable on different time scales, driven by both predictable and unpredictable elements.

For photoautotrophs, the ability to perceive the variations in the light regime and properly adjust and respond to such changes is critical to their survival. Indeed, there are a number of physiological mechanisms to cope with light regime variations that occur on different time scales, such as non-photochemical quenching, adjustment of pigment composition and content, and altering the composition and concentration of other components of the photosynthetic apparatus (Müller et al., 2001; Dubinsky and Stambler, 2009). In this study, we focus on the intra-day adjustments and responses of the phytoplankton occurring on the surface of the northern South China Sea (SCS). The South China Sea, the world's largest tropical marginal sea, plays important roles in regulating regional climate and biogeochemical cycles owing to its vast area and volume (Zhai et al., 2013). The shelf of the SCS is influenced by river inputs and is nutrient-rich. In contrast, its wide basin area is permanently stratified, depleted in surface nutrients, and contains low surface phytoplankton biomass (Tseng et al., 2005; Du et al., 2017), typical of the oligotrophic oceans. The surface phytoplankton community in the SCS basin area is dominated by pico-cyanobacteria, *Prochlorococcus* and *Synechococcus*, in the summer (Xiao et al., 2018). Due to its location in the tropical region, the incident solar radiation in the SCS was high, with surface photosynthetically active radiation at noon over  $2,000 \mu\text{mol quanta m}^{-2} \text{s}^{-1}$  on a clear day (Xie et al., 2018). Additionally, intensively stratified upper layer in warmed regions constrains the vertical mixing path of phytoplankton close to the sea surface, thus exposing phytoplankton to a high level of solar radiation (Gao et al., 2012). Therefore, dealing effectively with high light exposure, combined with a limited nutrient supply is critical for their survival (Mella-Flores et al., 2012; Murphy et al., 2017; Xie et al., 2018).

Here, we explored the diurnal patterns of photophysiological characteristics of phytoplankton in the northern South China Sea. Through comparing results obtained at different stations, we tried to identify the key environmental factors determining the diurnal variations of photophysiological characteristics on the intra-day time scale and found that the surface phytoplankton community in the oligotrophic SCS were able to maintain photosynthetic potential even with PSII photoinactivation.

## MATERIALS AND METHODS

### Study Sites and Sampling

Our research was conducted during an oceanographic expedition to the northern SCS aboard the R/V Dongfanghong 2 in the summer of 2017 (July 11 – August 11, 2017). The northern SCS is characterized by warm ( $\sim 23\text{--}31^\circ\text{C}$ ), oligotrophic, and stratified surface waters, with the mixed layer depth being between 20 and 40 m during most of the year (Tseng et al., 2005; Li et al., 2020 and the references therein). The whole cruise consists of 63 water-sampling stations, and our experiments were carried out at three stations (SEATS, DC2, and DC6; **Figure 1**) where the research vessel remained on each station for more than 24 h (**Table 1**).

For nutrient measurements (see below), seawater samples were collected using a CTD-rosette equipped with 10 L acid-cleaned Niskin bottles. Hydrological parameters, including pressure, salinity, and temperature, were measured using a Seabird CTD. The mixed layer depth (MLD) was calculated from the temperature profiles, with the criterion being  $>0.8^\circ\text{C}$  difference from the sea surface temperature (SST) (Kara et al., 2000). Additionally, surface seawater samples were collected with a 10 L acid-cleaned plastic bucket at different times of the day, then transferred to 10 L acid-cleaned polycarbonate carboys and immediately taken to the onboard laboratory for active Chl *a* fluorescence and phytoplankton pigment analyses (see below).

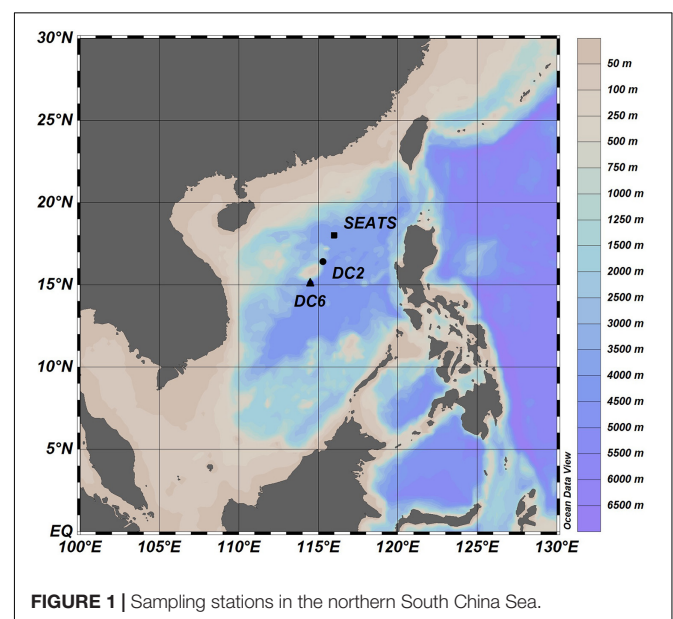


**FIGURE 1 |** Sampling stations in the northern South China Sea.

**TABLE 1** | Physical and chemical conditions at the sampling stations.

Station	Longitude	Latitude	Date	SST	SSS	Weather	Maximal PAR	Total Chl- <i>a</i>	Surface DIN	Surface SRP	DIN at 100 m	SRP at 100 m	MLD
				(°C)			( $\mu\text{mol quanta m}^{-2} \text{s}^{-1}$ )	( $\text{mg m}^{-3}$ )	( $\mu\text{mol L}^{-1}$ )	(m)			
SEATS	115.6°E	17.6°N	Jul 26, 2017	29.5	33.6	Cloudy, rainy	1,000	0.129	BLQ	BLQ	6.655	0.452	40
DC2	115.3°E	16.4°N	Aug 2, 2017	28.2	33.5	Sunny	>2,000	0.093	BLQ	BLQ	9.921	0.643	33
DC6	114.5°E	15.1°N	Aug 4, 2017	29.2	33.4	Sunny	>2,000	0.108	BLQ	BLQ	6.338	0.452	22

SST, sea surface temperature; SSS, sea surface salinity; DIN, dissolved inorganic nitrogen; SRP, soluble reactive phosphate; MLD, mixed layer depth.

The incident solar irradiance was measured by a portable LI-COR 2 $\pi$  PAR sensor (PMA2100, Solar light, United States). The PAR sensor is calibrated with a continuous solar irradiance monitor (SOLAR-2UV, TianNuo HuanNeng, China) which is set up on the roof of our experimental building and is routinely calibrated by the manufacturer. Additionally, we utilized satellite-measured daily PAR and a simple model to simulate the diurnal pattern of incident solar irradiance (Iqbal, 1983; Sung et al., 2015; see Supplementary Information for further details).

## Nutrients

Nutrient concentrations were analyzed onboard using a four-channel, continuous-flow Technicon AA3 Auto-Analyzer (Bran+Lube, GmbH, Germany). The concentrations of dissolved inorganic nitrogen (DIN, nitrate + nitrite), soluble reactive phosphate (SRP), and silicate were measured using standard colorimetric methods. The limits of quantification for DIN, SRP, and silicate are 0.1, 0.08, and 0.16  $\mu\text{mol L}^{-1}$ , and the analytical precision was better than 1% for DIN, 2% for SRP, and 2.5% for silicate, respectively. More details are described in Han et al. (2012).

## Phytoplankton Pigments

The concentrations of phytoplankton pigments were analyzed using high-performance liquid chromatography (HPLC). The sampling and analytical procedures for the HPLC analysis generally followed the protocol of Huang et al. (2010). Briefly, 6–10 L of seawater was filtered onto glass-fiber filters (diameter 25 mm, pore size 0.7  $\mu\text{m}$ , Whatman GF/F). The filters were preserved in liquid nitrogen until analysis. The filter was submerged in 1 ml of *N,N*-dimethylformamide (DMF) for 1 h in the dark at  $-20^\circ\text{C}$ . An aliquot (600  $\mu\text{L}$ ) of the DMF containing the extracted pigments was then mixed (1:1) with 1 M ammonium acetate. The pigments in the mixture after the removal of filter debris were analyzed using an UltiMate 3000 high-performance liquid chromatography system (Thermo Fisher Scientific, United States). The pigments were identified by the retention times and quantified using peak areas with standard curve calibration. Quantification was performed with standards purchased from DHI Water and Environment, Hørsholm, Denmark. Chemotaxonomic analysis was carried out using the CHEMTAX program (Mackey et al., 1996), which gave the proportions of nine phytoplankton classes [Dinoflagellates, Diatoms, Haptophytes (type 8), Haptophytes (type 6),

Cryptophytes, Chlorophytes, Prasinophytes, *Synechococcus*, and *Prochlorococcus*]. Although CHEMTAX only allowed identification of *Synechococcus* and *Prochlorococcus* among cyanobacteria, neglecting other cyanobacterial genera should not affect our main results and conclusions, because their biomass is extremely low in this region (Tseng et al., 2015).

## Active Chl *a* Fluorometry

Since we did not have access to the most widely used active Chl *a* fluorometry technique in field investigations, namely, fast repetition rate fluorometry (FRRF) (Kolber et al., 1998), which has a high measuring sensitivity that is best suitable for the low Chl *a* concentration found in large areas of the oceans, our variable fluorescence data were obtained using a Multiple Excitation Wavelength Chlorophyll Fluorescence Analyzer (multi-color-PAM, Walz, German). To satisfy the Chl *a* concentration requirement of the multi-color-PAM, phytoplankton cells were concentrated before measurement (Bailleul et al., 2017). Water samples (1,000 mL) were filtered through Nucleopore membrane filters (0.4 or 0.8  $\mu\text{m}$  pore-size) by gravity or under a very low vacuum ( $<0.3$  kPa). Cells were resuspended in 2 mL of the original seawater sample by soaking and gentle shaking in a 50-mL polypropylene centrifuge tube. The process was repeated two to four times. The cell enrichment procedure was typically finished within 0.5 h in the onboard laboratory where the temperature was similar to the SST of the study sites and light intensity during the enrichment process was  $<10$   $\mu\text{mol quanta m}^{-2} \text{s}^{-1}$ . After cell enrichment, cells were kept in the darkness for 10 min. Keeping cells under low light intensity for 30 min (during the cell enrichment) and subsequently in the darkness for 10 min allows photosynthetic apparatus relaxation from potential non-photochemical quenching processes but not recovery from photodamage (Campbell and Tyystjärvi, 2012). Subsequently, the maximum quantum yield of PSII ( $F_v/F_m$ ) was determined:

$$F_v/F_m = (F_m - F_o) / F_m, \quad (1)$$

where  $F_o$  and  $F_m$  are the dark-acclimated minimum and maximum fluorescence, respectively. The values of  $F_v/F_m$  reported in this study were within expected values (Suggett et al., 2009) and comparable to those reported in other research conducted in the northern SCS (Xie et al., 2018), so the process of cell enrichment appeared to not significantly affect the phytoplankton photophysiological characteristics. After

measurement of  $F_v/F_m$ , the functional absorption cross-section of PSII was determined according to the procedures of Schreiber et al. (2012) and the manufacturer's manual. The definition of the functional absorption cross section of PSII was introduced by Ley and Mauzerall (1982) and is used to quantify the light absorption and utilization potential of PSII. This parameter has been widely and readily measured using FRRf and is usually denoted as  $\sigma_{PSII}$  in the literature (Kolber et al., 1998; Suggett et al., 2009). The correct determination of the functional absorption cross section of PSII relies on the high time-resolution record of the fluorescence rise kinetics induced by strong light, which is achieved by FRRf and PAM using different approaches. Following the suggestions of the manufacturers of the multi-color-PAM (Schreiber et al., 2012), the functional absorption cross section of PSII determined by multi-color-PAM is denoted as Sigma(II) to highlight its difference from  $\sigma_{PSII}$ . In terms of data interpretation, Sigma(II) is only valid for the reference state in which it is measured and any changes of PSII efficiency occurring, e.g., during illumination are assumed to be covered by corresponding changes in the effective PSII photochemical efficiency, whereas  $\sigma_{PSII}$  changes during illumination (Schreiber et al., 2012).

Determination of relative electron transport rate (rETR) relied on measurement of effective photochemical efficiency of PSII ( $\Phi_{PSII}$ ).  $\Phi_{PSII}$  was successively measured at eight levels of actinic light with intensity (E) being 0, 8, 26, 57, 113, 218, 350, and 508  $\mu\text{mol quanta m}^{-2} \text{s}^{-1}$ , respectively. Cells were allowed to acclimate to each light level for 3 min before  $\Phi_{PSII}$  measurements (Suggett et al., 2007):

$$\Phi_{PSII} = (F_m' - F') / F_m', \quad (2)$$

where  $F_m'$  is the light-adapted maximum fluorescence and  $F'$  is the stable fluorescence under actinic light. rETR at each actinic light level (E) was calculated as Ralph and Gademann (2005):

$$\text{rETR} = E \times \Phi_{PSII} \quad (3)$$

The light response curve of rETR was analyzed according to the model proposed by Eilers and Peeters (1988):

$$\text{rETR} = \frac{E}{a \times E^2 + b \times E + c}, \quad (4)$$

where a, b and c are parameters that were obtained through non-linear least squares regression using R (version 4.0.5). Photosynthetic parameters including light use efficiency ( $\alpha$ ), rETR maximum ( $\text{rETR}_{\text{max}}$ ), and light saturation point ( $E_k$ ) were calculated as:

$$\alpha = \frac{1}{c} \quad (5)$$

$$\text{rETR}_{\text{max}} = \frac{1}{b + 2\sqrt{ac}} \quad (6)$$

$$E_k = \frac{c}{b + 2\sqrt{ac}} \quad (7)$$

During the  $\Phi_{PSII}$  measurements,  $F_o'$ , the light-acclimated minimum fluorescence was also measured, based on which

we calculated the light-acclimated maximum photochemical efficiency ( $F_v'/F_m'$ ) and the photochemical quenching (qP) at each level of actinic light:

$$F_v'/F_m' = (F_m' - F_o') / F_m' \quad (8)$$

$$qP = (F_m' - F) / (F_m' - F_o') \quad (9)$$

From Equations 1, 8, 9, we can get:

$$\Phi_{PSII} = F_v'/F_m' \times qP \quad (10)$$

Blue light (440 nm) was selected as the measuring light to obtain the active Chl *a* fluorescence data. Sample temperature in the fluorometer during the measurements was maintained at the corresponding *in situ* temperature using a US-T temperature control unit (Walz, Germany). Two independent samples were used for active Chl *a* fluorescence measurement at each time point.

## Statistical Analyses

A Generalized Additive Model (GAM) was used to analyze the diurnal variations of PAM-derived parameters in which time was treated as the covariate and the PAM-derived parameter was treated as the dependent variable. This helps to highlight and compare the patterns of diurnal variations between stations. Additionally, to quantitatively compare the patterns of diurnal variation between stations, Pearson's correlations were used. Because sampling time points were different between stations, the calculations of Pearson's correlations were based on the values predicted by GAM. All statistical analyses were completed using R (version 4.0.5), and the core package was "mgcv" (version 1.8–34). **Figure 1** was created using Ocean Data View (version 5.4.0), and other figures were created in R (version 4.0.5) using packages "ggplot2" (version 3.3.3), "ggpubr" (version 0.4.0), and "ggtext" (version 0.1.1).

## RESULTS

### Environmental Conditions of the Study Sites

Environmental conditions were similar among the three stations during the experimental period (**Table 1**). The sea surface temperature (SST) was  $\sim 29^\circ\text{C}$ , the sea surface salinity was  $\sim 33.5$ , and the mixed layer depth (MLD) was less than 40 m across all three stations. The concentrations of both DIN and SRP in the surface waters were below the limit of quantification ( $0.1 \mu\text{mol L}^{-1}$  for DIN;  $0.08 \mu\text{mol L}^{-1}$  for SRP), and the silicate concentration was about  $2 \mu\text{mol L}^{-1}$  at all three stations. There existed, however, one readily noticeable and significant difference between different stations, that is, the weather conditions. At station SEATS, the experiment was conducted on a cloudy and rainy day with the daily maximum of surface PAR below  $1,000 \mu\text{mol quanta m}^{-2} \text{s}^{-1}$ , whereas experiments at stations DC2 and DC6 were carried out on sunny days with the surface

PAR maxima higher than  $2,000 \mu\text{mol quanta m}^{-2} \text{s}^{-1}$ . This difference was also reflected in the values of daily PAR which were separately 30.37, 57.24, and  $50.95 \text{ Einstein m}^{-2} \text{d}^{-1}$  at stations SEATS, DC2, and DC6 (**Supplementary Figure 1** and **Supplementary Table 1**).

## Phytoplankton Pigments and Community Structures

The total Chl *a* (chlorophyll *a* + divinyl-chlorophyll *a*) concentrations of the surface waters were similar between stations, at a level of  $\sim 0.1 \text{ mg m}^{-3}$  (**Table 1**). The surface phytoplankton assemblages were dominated by *Prochlorococcus* and *Synechococcus* (**Figure 2**) regardless of station and sampling time, accounting for 63–81% and 12–31%, respectively, of the total Chl *a*. However, the diurnal variation of phytoplankton community structure at station SEATS (**Figure 2A**) was different from those at stations DC2 (**Figure 2B**) and DC6 (**Figure 2C**). Specifically, the phytoplankton community composition at station SEATS varied only slightly over the course of the diurnal cycle with no obvious pattern (**Figure 2A**), but at both station DC2 (**Figure 2B**) and station DC6 (**Figure 2C**), the proportion of *Prochlorococcus* increased gradually during the morning, reaching a daily maximum before noon and thereafter steadily decreasing until the end of the day. Additionally, highly negative correlations between proportions of *Prochlorococcus* and *Synechococcus* were detected across all stations (Pearson's correlations were  $-0.90$ ,  $-0.98$ , and  $-0.98$  at SEATS, DC2, and DC6). The proportions of phytoplankton groups other than *Prochlorococcus* and *Synechococcus* were less than 9% regardless of sampling station and time (**Figure 2**).

## $F_v/F_m$ and Sigma(II)

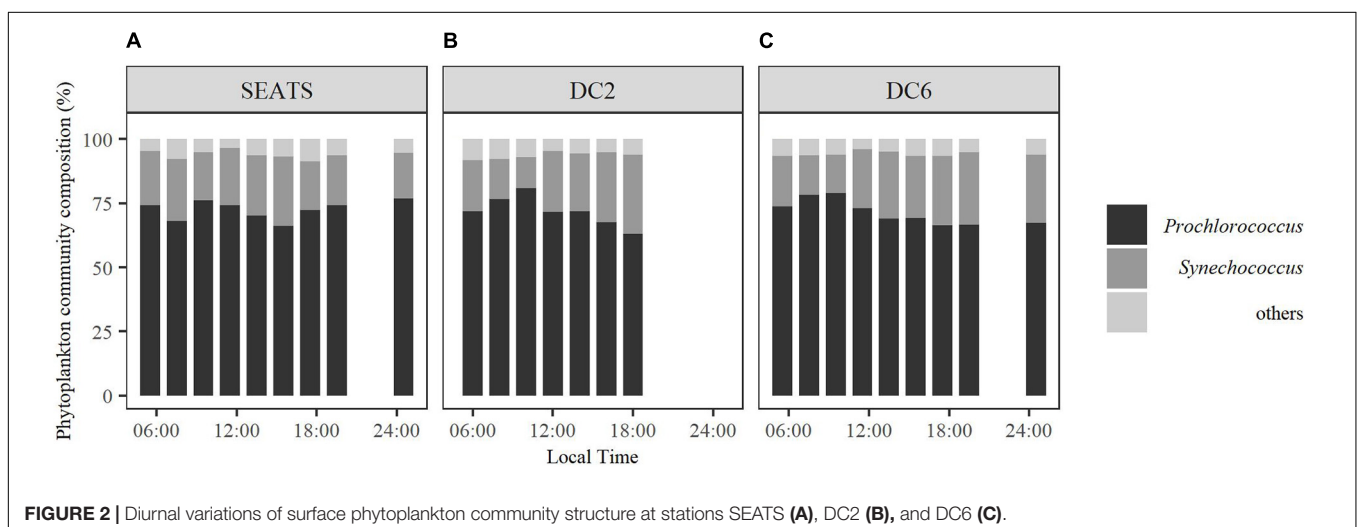
The values of maximum quantum yield of PSII ( $F_v/F_m$ ) showed no obvious difference at the beginning of the experiments between stations ( $\sim 0.5$ ), but patterns diverged over the course of the day (**Figure 3** and **Supplementary Figure 2**). At station SEATS (**Figure 3A**),  $F_v/F_m$  values fluctuated only slightly within

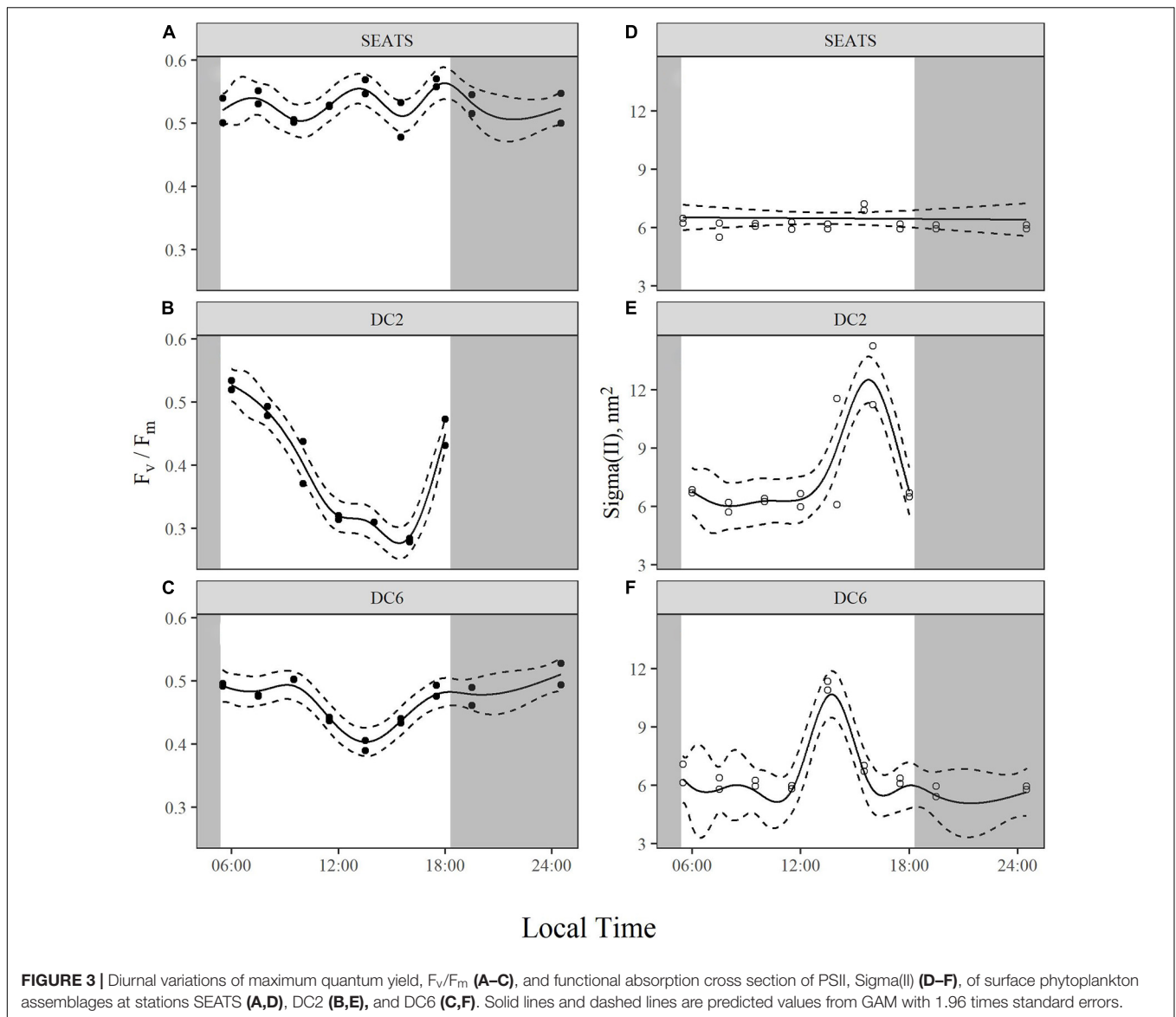
the range of 0.48–0.57. However, at stations DC2 (**Figure 3B**) and DC6 (**Figure 3C**),  $F_v/F_m$  steadily declined in the morning and dropped to a daily minimum around 14:00 with values of 0.28 at station DC2 and 0.39 at station DC6. Subsequently,  $F_v/F_m$  in these two stations recovered and finally returned to values of  $\sim 0.5$  at the end of the experiments. Such similarity of diurnal variation patterns between stations DC2 and DC6 was also illustrated by the high correlation (Pearson's correlation, 0.82), which is not found between SEATS and DC2 (Pearson's correlation,  $-0.001$ ) or SEATS and DC6 (Pearson's correlation,  $-0.37$ ).

There were similar patterns of diurnal variations of functional absorption cross-section of PSII [Sigma(II)] across three stations (**Figures 3D–F**). During most of the daytime, the values of Sigma(II) were similar ( $\sim 6 \text{ nm}^2$ ), but at around 14:00 the values of Sigma(II) were apparently higher than those measured at other time points. Such a Sigma(II) peak was more prominent at stations DC2 (**Figure 3E**) and DC6 (**Figure 3F**) ( $\sim 11 \text{ nm}^2$ ) than at the station SEATS ( $\sim 7 \text{ nm}^2$ ) (**Figure 3D**).

## The Diurnal Variations of rETR

Over the course of the diurnal cycle, variations in the light dependence of rETR were observed at all stations (**Figure 4**). These variations were quantitatively described by the changes of the parameters  $rETR_{\text{max}}$  and  $E_k$  (**Figure 5** and **Supplementary Figures 3, 4**). Generally,  $rETR_{\text{max}}$  increased after sunrise, reached maximal values around noon, and decreased afterward at all stations (**Figures 5A–C**). However, the timing of the peak and the magnitude of the diurnal variation of  $rETR_{\text{max}}$  were different between stations. At stations SEATS (**Figure 5A**) and DC6 (**Figure 5C**), the daily maximal value of  $rETR_{\text{max}}$  was observed at  $\sim 12:00$ , but was observed at 10:00 at station DC2 (**Figure 5B**). In addition, the changing range of  $rETR_{\text{max}}$  was  $30 \sim 100 \text{ a.u.}$  (arbitrary units) at stations SEATS and DC6, but the corresponding range was narrower at station DC2, varying between 40 and 80 a.u. The  $E_k$  showed similar patterns of diurnal variations at all stations, with values ranging between  $\sim 50$  and  $\sim 200 \mu\text{mol quanta m}^{-2} \text{s}^{-1}$ , and the daily maxima were all





achieved at midday (Figures 5D–F). Additionally, only at station DC2 (Figure 5E), was a second peak of  $E_k$  found at around 16:00.

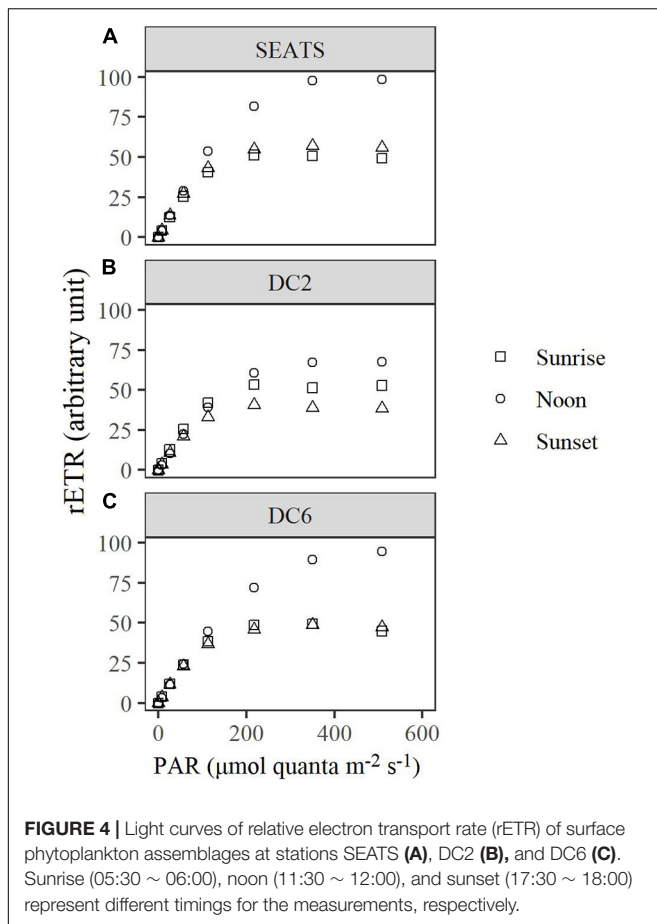
### $F_v'/F_m'$ and qP

Note that the values of  $F_v'/F_m'$  and qP shown in Figure 6 and (Supplementary Figures 5, 6) and analyzed below were obtained under an actinic light intensity of  $350 \mu\text{mol quanta m}^{-2} \text{s}^{-1}$  rather than *in situ* light intensity at each time point. Measured  $F_v'/F_m'$  exhibited similar values at the beginning of the day at all three stations, but the subsequent diurnal variation patterns were different between stations (Figures 6A–C). At station SEATS (Figure 6A),  $F_v'/F_m'$  increased in the morning, reached the daily maximum at around 13:30, and decreased gradually afterward. However, the values of  $F_v'/F_m'$  at station DC2 (Figure 6B) decreased gradually after the first time point, dropped to a minimum at around 14:00, and then recovered

afterward. At station DC6 (Figure 6C), the diurnal pattern of  $F_v'/F_m'$  was similar to that at the SEATS station, except the daily maximum was reached earlier (at  $\sim 10:00$ ). The values of qP at stations SEATS (Figure 6D), DC2 (Figure 6E), and DC6 (Figure 6F) evolved during the daytime in a similar way. At the first time point (around 05:30–06:00), qP values were around 0.4, gradually increased to approximately 0.8 at midday, and decreased afterward.

## DISCUSSION

In the present study, we investigated the diurnal patterns of photophysiology of cyanobacteria-dominated phytoplankton at three stations in the northern SCS at which environmental conditions were similar except for the contrasting light regimes at the time of sampling. We could thus ascertain the effects of



the light regime through the comparisons of the observations between stations.

The DIN and SPR were depleted (Table 1) and previous studies indicate that the primary limitation to phytoplankton growth in the northern SCS is the availability of nutrients (Lee Chen, 2005; Lee Chen and Chen, 2006), but the values of  $F_v/F_m$  at dawn were as high as 0.5 at all stations (Figure 3). Such values were comparable to or slightly less than those reported in laboratory experiments in which *Prochlorococcus* or *Synechococcus* were cultured with replete nutrient availability (Bruyant et al., 2005; Mella-Flores et al., 2012; Murphy et al., 2017). It has been shown that phytoplankton are able to maintain balanced growth and high  $F_v/F_m$  in a stable environment with continuously limited nutrient supply (Parkhill et al., 2001; Suggett et al., 2009). Therefore, our results indicated that although nutrient supply was limited, phytoplankton were likely under balanced growth.

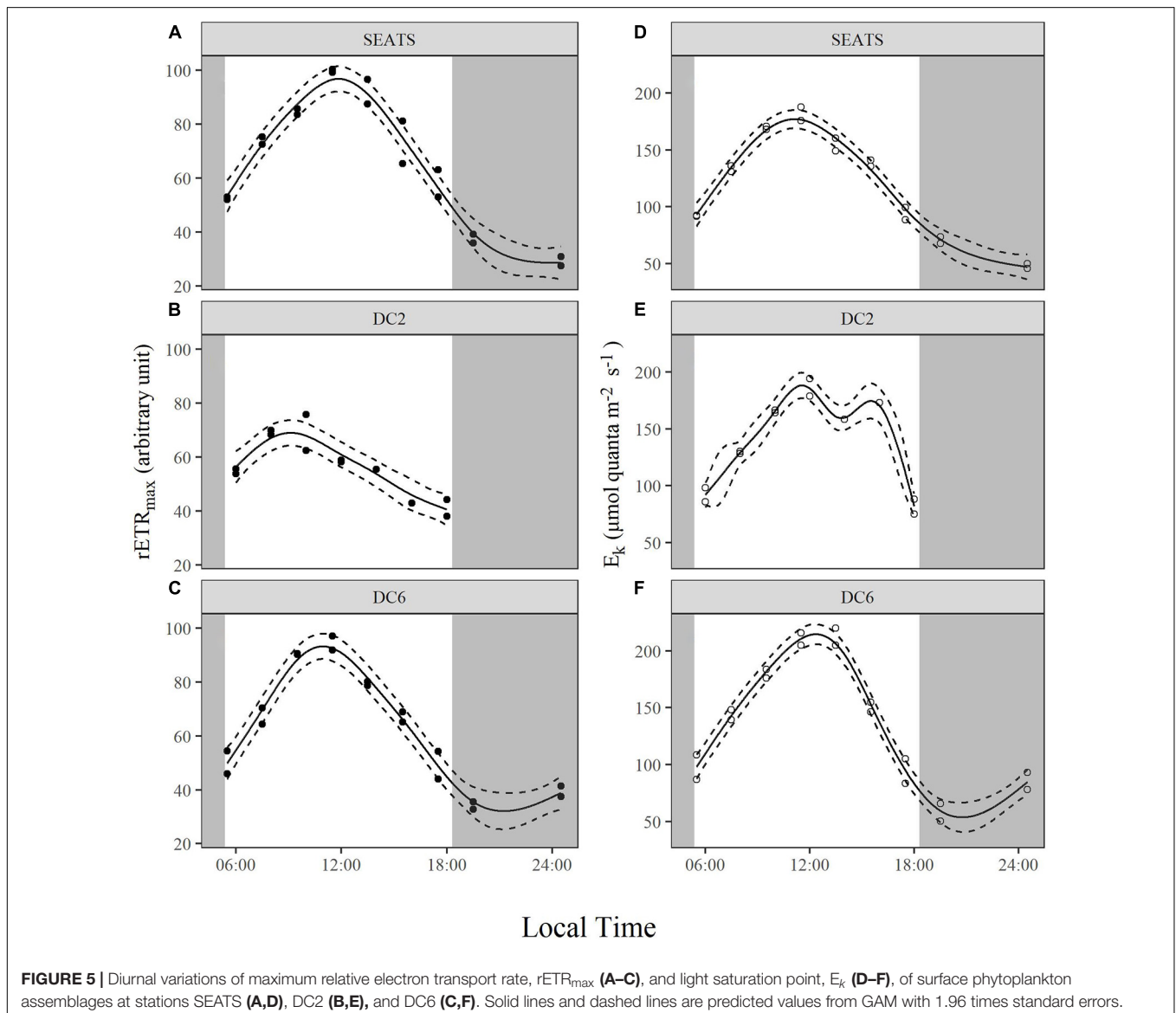
Across the course of the day,  $F_v/F_m$  values at SEATS were relatively constant with the daily maximum of surface PAR being less than 1,000 quanta  $m^{-2} s^{-1}$ , whereas we observed an obvious drop in  $F_v/F_m$  around midday with the maximum surface PAR exceeding 2,000  $\mu mol quanta m^{-2} s^{-1}$  at DC2 and DC6 (Figure 2 and Table 1). Additionally, compared to station SEATS, the shallower MLD at stations DC2 and DC6 might also increase the mean light intensity received

by phytoplankton within the upper mixed layer (Table 1). Decreasing  $F_v/F_m$  is a typical indicator of photoinactivation of PSII induced by high light, which is accompanied by the damage and degradation of the D1 protein in PSII (Ragni et al., 2010; Wu et al., 2011; Campbell and Tyystjärvi, 2012; McKew et al., 2013; Murphy et al., 2017; Ni et al., 2017; Campbell and Serôdio, 2020). In addition, salinity, nutrients, and pH of the seawater and the operation of photoprotective non-photochemical quenching (NPQ) under circadian clocks can also affect the value of  $F_v/F_m$  (Berman-Frank et al., 2001; Dijkman and Kromkamp, 2006; Fu et al., 2007; Suggett et al., 2009). During the experimental period, nutrient and salinity conditions were comparable between the three stations and  $F_v/F_m$  values at dawn were similar, so if the midday drop of  $F_v/F_m$  at stations DC2 and DC6 had been related to the salinity or nutrient status of phytoplankton cells (Behrenfeld and Kolber, 1999; Behrenfeld et al., 2006; Xie et al., 2018), we would have observed a similar phenomenon at station SEATS. Additionally, phytoplankton community structures were highly similar across three stations, so if a circadian clock or photoprotective NPQ had played a role, we also would have observed a similar midday  $F_v/F_m$  drop at station SEATS. Furthermore, keeping phytoplankton samples in low light and darkness before active Chl *a* fluorescence measurement should relax most of the photoprotective NPQ (Campbell and Tyystjärvi, 2012), which also suggests that photoprotective NPQ would not explain our observations. Although we did not measure the parameters of carbonate chemistry, previous studies indicate that these values would be similar across this region (Chen et al., 2006; Du et al., 2020), so the differences in the diurnal patterns of  $F_v/F_m$  are unlikely to be related to the seawater pH. However, phytoplankton cells at stations DC2 and DC6 were definitely exposed to higher light intensity. Therefore, we argue that decreasing midday  $F_v/F_m$  values at stations DC2 and DC6 were caused by high light, indicating photoinactivation of PSII. Compared to station DC6, light intensity was higher at station DC2, corresponding to the more intense photoinactivation (lower  $F_v/F_m$  around noon) found at station DC2 (Supplementary Table 1 and Supplementary Figure 1). Additionally, at both stations DC2 and DC6, daily minima of  $F_v/F_m$  slightly lagged behind the daily maxima of PAR, conforming with accumulative effects of photoinactivation (Supplementary Figure 1). Murphy et al. (2017), through laboratory experiments with *Prochlorococcus* and *Synechococcus*, showed that under low to moderate light, photoinactivation of PSII is mainly caused by absorbance of short-wavelength light (blue light and UV) by the  $Mn_4Ca$  cluster in the PSII oxygen-evolving complex, whereas under high excitation pressure, ROS formation is the dominant mechanism leading to photoinactivation. As found in our results, under low to moderate light (at station SEATS), a relatively stable  $F_v/F_m$  might be a reflection of a balance between PSII damage and repair (no net photoinactivation), whereas under high light pressure (at DC2 and DC6), cells produced ROS not only can damage PSII directly but also inhibit repair process (Mella-Flores et al., 2012; Murphy et al., 2017), ultimately leading to net photoinactivation. Laboratory experiments indicate that compared to *Synechococcus*, *Prochlorococcus* is more susceptible

to photoinactivation and invests fewer resources to repair of inactivated PSII, which might be a tradeoff for a high acquisition of nutrients (Mella-Flores et al., 2012; Murphy et al., 2017). Nevertheless, at both stations DC2 and DC6,  $F_v/F_m$  values recovered to about 0.5 around dusk, indicating the relief of photoinactivation. A midday drop in  $F_v/F_m$  on a clear day is recognized as a general phenomenon for natural phytoplankton communities living in the upper layer of the water column (Doblin et al., 2011; Xie et al., 2018; Schuback and Tortell, 2019; Xu et al., 2020).

Unlike  $F_v/F_m$ , Sigma(II) was relatively stable during most of the time at all three stations (Figure 2), though in another study conducted in the same area, light-acclimated  $\sigma_{PSII}$  (functional absorption cross section measured by FRRf) was negatively correlated to the incident irradiance intensity (Xie et al., 2018). Considering the difference in pre-treatment of samples

(dark acclimation vs. no dark acclimation), such inconsistency suggests that the decrease in PSII functional absorption cross section induced by high light might be quickly reversed by dark acclimation. Such conjecture is consistent with the results from another study in which both dark-acclimated and light-acclimated  $\sigma_{PSII}$  were simultaneously measured (Schuback and Tortell, 2019). In this study,  $\sigma_{PSII}$  is relatively stable during the day and  $\sigma_{PSII}'$  displays a midday minimum. In our study, superimposed on the mostly stable Sigma(II) were abnormally high values near noon at all three stations (Figures 2D–F), especially at stations DC2 and DC6. In addition to some unclear physiological basis for such phenomenon, we have to consider the possibility that the seemingly abnormal peaks at noon might relate to some technical issue. Because the intensive photoinactivation of PSII at noon makes the curve of fluorescence induction kinetics quite flat (data not shown), this



might affect the calculation of  $\Sigma(II)$  which relies on the model fitting of the curve.

Although cyanobacteria-dominated phytoplankton at stations DC2 and DC6 presented as being photoinactivated around noon, they also showed a midday peak of  $rETR_{max}$  as did the phytoplankton at station SEATS. Photosynthetic electron transport chains supply the reductant and energy for the dark reactions of photosynthesis, so the parameter,  $rETR_{max}$ , partially reflects the photosynthetic potential (Ralph and Gademann, 2005). Therefore, our results suggest that phytoplankton in the oligotrophic SCS could maintain photosynthetic potential even under the influence of photoinactivation of PSII. Additionally, based on Figure 4 and Equation 3,  $rETR_{max}$  directly reflects the ability of cells to maintain effective photochemical efficiency ( $\Phi_{PSII}$ ) at high light. Furthermore, the value of  $\Phi_{PSII}$  can be decomposed into  $F_v'/F_m'$  and qP (Equations 8–10). In the present

study, the diurnal patterns of  $rETR_{max}$  were mainly controlled by qP rather than  $F_v'/F_m'$  (Figures 5A–C, 6). At each study site, the diurnal variations of  $rETR_{max}$  mimicked those of qP, and the daily peak of  $rETR_{max}$  was amplified at stations SEATS and DC6 but offset and slightly advanced at station DC2 via changes in  $F_v'/F_m'$ . Higher incident solar irradiance at station DC2, which resulted in greater photoinactivation, might explain why the diurnal variations of  $F_v'/F_m'$  at station DC2 were different from those at stations SEATS and DC6 (Figures 6A–C and Supplementary Figure 6). In terms of qP, higher values, generally, reflect a situation in which PSII downstream is in a more oxidizing state, which requires active electron-consuming reactions downstream of PSII, such as the dark reactions of photosynthesis (Falkowski and Raven, 2007). In *Prochlorococcus* and *Synechococcus*, the expression of the key carbon fixation enzyme, ribulose biphosphate carboxylase/oxygenase (Rubisco),

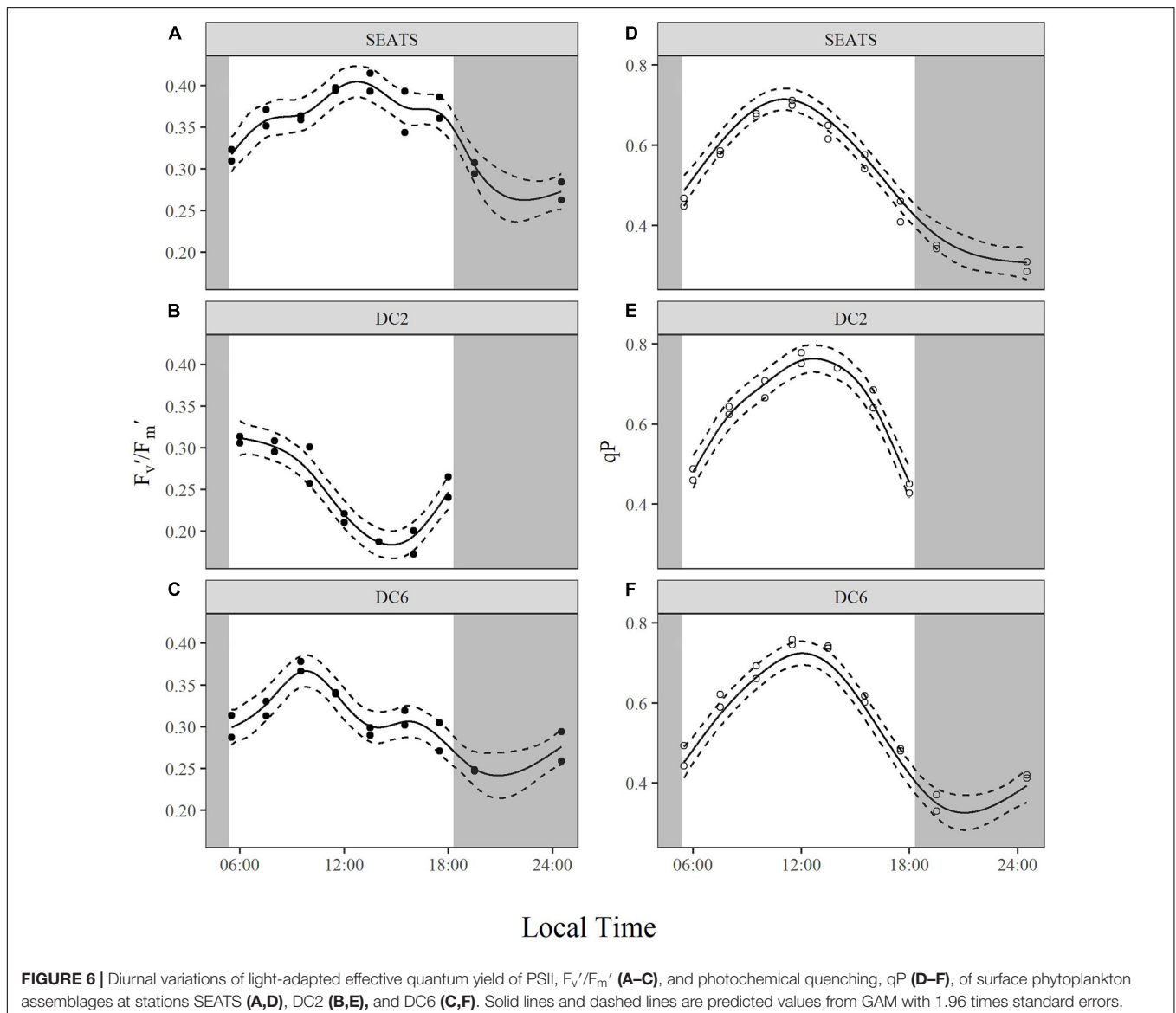


**FIGURE 6** | Diurnal variations of light-adapted effective quantum yield of PSII,  $F_v'/F_m'$  (A–C), and photochemical quenching, qP (D–F), of surface phytoplankton assemblages at stations SEATS (A,D), DC2 (B,E), and DC6 (C,F). Solid lines and dashed lines are predicted values from GAM with 1.96 times standard errors.

has been shown to be partially controlled by an endogenous circadian clock (Pichard et al., 1996; Wyman, 1999; Paul et al., 2000), especially for *Synechococcus* whose circadian clock can remain after cells are transferred to the continuous light regime (Pattanayak and Rust, 2014; Cohen and Golden, 2015). In addition to the dark reactions, other electron-consuming mechanisms may also contribute to the midday qP peak. These include components such as the plastid terminal oxidase (PTOX) and alternative oxidase (AOX) (McDonald and Vanlerberghe, 2005; Berg et al., 2011), whose activities also show a circadian rhythm. In addition, cyanobacteria are known for their ability to adjust the energy allocation between PSII and PSI (state transition) (Campbell et al., 1998). Several electron consuming processes rely on the operation of PSI (Mullineaux, 2014a,b), and PSI is more tolerant to high light than PSII (Tikkanen et al., 2014), so state transitions may play a role in maintaining the midday photosynthetic potential through channeling more energy to PSI. Overall, our results indicated that the  $rETR_{max}$ , a proxy for photosynthetic potential, presented as being unimodal with a peak around midday, which might be mainly controlled by endogenous circadian clock, and could maintain high values under the influence of high light-induced photoinactivation.

The  $rETR_{max}$  was interpreted as the photosynthetic potential here, but  $rETR$  is not necessarily proportional to  $O_2$  evolution or carbon fixation (Schuback et al., 2016; Schuback and Tortell, 2019).  $rETR$  is a simplified parameter quantifying the overall linear electron transport rate. From electron transport to carbon fixation, the existence of such electron consumption mechanisms as nitrate reduction, sulfate reduction and the water-water cycles (Mullineaux, 2014a,b; Raven et al., 2020) affect the ratio of electron transport to carbon fixation. The inconsistency between electron transport and carbon fixation might cause their patterns of diurnal variation to be different from each other (Schuback et al., 2016; Xie et al., 2018; Schuback and Tortell, 2019). In addition, both *Prochlorococcus* and *Synechococcus* contain diverse ecotypes/subclusters that show different niche adaptation (Rocap et al., 2002; Scanlan et al., 2009). Generally, in the SCS, the *Synechococcus* subcluster 5.2 dominates the coastal cyanobacteria community, and the high-light ecotypes of *Prochlorococcus* and the subcluster 5.1 of *Synechococcus* are the major ecotype/subcluster in the open

water (Jing and Liu, 2012; Xia et al., 2015). However, there are spatially and temporally variations in the ecotype/subcluster composition (Jing and Liu, 2012; Xia et al., 2015; Singh and Bhadury, 2018). Therefore, concomitantly determining the ecotype/subcluster composition will improve our understanding of the diurnal patterns of phytoplankton photophysiological characteristics and its relationship to the ecotype/subcluster composition in the future.

## DATA AVAILABILITY STATEMENT

The raw data supporting the conclusions of this article will be made available by the authors, without undue reservation.

## AUTHOR CONTRIBUTIONS

XY and KG designed the experiment. XY, DZ, and JS carried out the experiment. XY, KG, and JB analyzed the data and wrote the manuscript. All authors contributed to the article and approved the submitted version.

## FUNDING

The study was supported by National Natural Science Foundation of China (41720104005, 41890803, and 41721005).

## ACKNOWLEDGMENTS

The authors would like to thank the laboratory engineers Xianglan Zeng and Wenyan Zhao for their logistic and technical supports.

## SUPPLEMENTARY MATERIAL

The Supplementary Material for this article can be found online at: <https://www.frontiersin.org/articles/10.3389/fmars.2021.736586/full#supplementary-material>

## REFERENCES

- Bailleul, B., Park, J., Brown, C. M., Bidle, K. D., Lee, S. H., and Falkowski, P. G. (2017). Direct measurements of the light dependence of gross photosynthesis and oxygen consumption in the ocean. *Limnol. Oceanogr.* 62, 1066–1079. doi: 10.1002/lno.10486
- Behrenfeld, M. J., and Kolber, Z. S. (1999). Widespread iron limitation of phytoplankton in the South Pacific Ocean. *Science* 283, 840–843. doi: 10.1126/science.283.5403.840
- Behrenfeld, M. J., Worthington, K., Sherrell, R. M., Chavez, F. P., Strutton, P., McPhaden, M., et al. (2006). Controls on tropical Pacific Ocean productivity revealed through nutrient stress diagnostics. *Nature* 442, 1025–1028. doi: 10.1038/nature05083
- Berg, G. M., Shrager, J., van Dijken, G., Mills, M. M., Arrigo, K. R., and Grossman, A. R. (2011). Responses of psbA, hli and ptox genes to changes in irradiance in marine *Synechococcus* and *Prochlorococcus*. *Aquat. Microb. Ecol.* 65, 1–14.
- Berman-Frank, I., Lundgren, P., Chen, Y.-B., Küpper, H., Kolber, Z., Bergman, B., et al. (2001). Segregation of nitrogen fixation and oxygenic photosynthesis in the marine cyanobacterium *Trichodesmium*. *Science* 294, 1534–1537. doi: 10.1126/science.1064082
- Bruyant, F., Babin, M., Genty, B., Prasil, O., Behrenfeld, M. J., Claustre, H., et al. (2005). Diel variations in the photosynthetic parameters of *Prochlorococcus* strain PCC 9511: combined effects of light and cell cycle. *Limnol. Oceanogr.* 50, 850–863. doi: 10.4319/lno.2005.50.3.0850
- Campbell, D., Hurry, V., Clarke, A. K., Gustafsson, P., and Öquist, G. (1998). Chlorophyll fluorescence analysis of cyanobacterial photosynthesis and acclimation. *Microbiol. Mol. Biol. Rev.* 62, 667–683. doi: 10.1128/MMBR.62.3.667-683.1998
- Campbell, D. A., and Seródio, J. (2020). “Photoinhibition of photosystem II in phytoplankton: processes and patterns,” in *Photosynthesis in Algae: Biochemical and Physiological Mechanisms*, eds A. W. D. Larkum, A. R. Grossman, and J. A. Raven (Cham: Springer International Publishing), 329–365.
- Campbell, D. A., and Tyystjärvi, E. (2012). Parameterization of photosystem II photoinactivation and repair. *Biochim. Biophys. Acta* 1817, 258–265. doi: 10.1016/j.bbabi.2011.04.010

- Chen, C.-T. A., Wang, S.-L., Chou, W.-C., and Sheu, D. D. (2006). Carbonate chemistry and projected future changes in pH and CaCO<sub>3</sub> saturation state of the South China Sea. *Mar. Chem.* 101, 277–305. doi: 10.1016/j.marchem.2006.01.007
- Cohen, S. E., and Golden, S. S. (2015). Circadian rhythms in cyanobacteria. *Microbiol. Mol. Biol. Rev.* 79, 373–385. doi: 10.1128/mmb.00036-15
- Doblin, M. A., Petrou, K. L., Shelly, K., Westwood, K., van den Enden, R., Wright, S., et al. (2011). Diel variation of chlorophyll-a fluorescence, phytoplankton pigments and productivity in the Sub-Antarctic and Polar Front Zones south of Tasmania, Australia. *Deep Sea Res. Part II Top. Stud. Oceanogr.* 58, 2189–2199. doi: 10.1016/j.dsr2.2011.05.021
- Dijkman, N. A., and Kromkamp, J. C. (2006). Photosynthetic characteristics of the phytoplankton in the scheldt estuary: community and single-cell fluorescence measurements. *Eur. J. Phycol.* 41, 425–434. doi: 10.1080/09670260600937791
- Du, C., Gan, J., Hui, C. R., Lu, Z., Zhao, X., Roberts, E., et al. (2020). Dynamics of dissolved inorganic carbon in the South China Sea: a modeling study. *Prog. Oceanogr.* 186:102367. doi: 10.1016/j.pocean.2020.102367
- Du, C., Liu, Z., Kao, S.-J., and Dai, M. (2017). Diapycnal fluxes of nutrients in an oligotrophic oceanic regime: the South China sea. *Geophys. Res. Lett.* 44, 11, 510–511, 518. doi: 10.1002/2017GL074921
- Dubinsky, Z., and Stambler, N. (2009). Photoacclimation processes in phytoplankton: mechanisms, consequences, and applications. *Aquat. Microb. Ecol.* 56, 163–176. doi: 10.3354/ame01345
- Eilers, P. H. C., and Peeters, J. C. H. (1988). A model for the relationship between light intensity and the rate of photosynthesis in phytoplankton. *Ecol. Model.* 42, 199–215. doi: 10.1016/0304-3800(88)90057-9
- Falkowski, P. G., and Raven, J. A. (2007). *Aquatic Photosynthesis*. Princeton, NJ: Princeton University Press.
- Field, C. B., Behrenfeld, M. J., Randerson, J. T., and Falkowski, P. (1998). Primary production of the biosphere: integrating terrestrial and oceanic components. *Science* 281, 237–240. doi: 10.1126/science.281.5374.237
- Fu, F.-X., Warner, M. E., Zhang, Y., Feng, Y., and Hutchins, D. A. (2007). Effects of increased temperature and CO<sub>2</sub> on photosynthesis, growth, and elemental ratios in marine *Synechococcus* and *Prochlorococcus* (Cyanobacteria). *J. Phycol.* 43, 485–496. doi: 10.1111/j.1529-8817.2007.00355.x
- Gao, K., Helbling, E. W., Häder, D. P., and Hutchins, D. A. (2012). Responses of marine primary producers to interactions between ocean acidification, solar radiation, and warming. *Mar. Ecol. Prog. Ser.* 470, 167–189. doi: 10.3354/meps10043
- Han, A., Dai, M., Kao, S.-J., Gan, J., Li, Q., Wang, L., et al. (2012). Nutrient dynamics and biological consumption in a large continental shelf system under the influence of both a river plume and coastal upwelling. *Limnol. Oceanogr.* 57, 486–502. doi: 10.4319/lo.2012.57.2.0486
- Huang, B., Hu, J., Xu, H., Cao, Z., and Wang, D. (2010). Phytoplankton community at warm eddies in the northern South China Sea in winter 2003/2004. *Deep Sea Res. Part II Top. Stud. Oceanogr.* 57, 1792–1798. doi: 10.1016/j.dsr2.2010.04.005
- Iqbal, M. (1983). *An Introduction to Solar Radiation*. New York, NY: Elsevier.
- Jing, H., and Liu, H. (2012). Phylogenetic composition of *Prochlorococcus* and *Synechococcus* in cold eddies of the South China Sea. *Aquat. Microb. Ecol.* 65, 207–219. doi: 10.3354/ame01546
- Kara, A. B., Rochford, P. A., and Hurlburt, H. E. (2000). An optimal definition for ocean mixed layer depth. *J. Geophys. Res.* 105, 16803–16821. doi: 10.1029/2000jc900072
- Kolber, Z. S., Prášil, O., and Falkowski, P. G. (1998). Measurements of variable chlorophyll fluorescence using fast repetition rate techniques: defining methodology and experimental protocols. *Biochim. Biophys. Acta* 1367, 88–106. doi: 10.1016/S0005-2728(98)00135-2
- Lee Chen, Y.-I. (2005). Spatial and seasonal variations of nitrate-based new production and primary production in the South China Sea. *Deep Sea Res. Part I Oceanogr. Res. Pap.* 52, 319–340. doi: 10.1016/j.dsr.2004.11.001
- Lee Chen, Y.-I., and Chen, H.-Y. (2006). Seasonal dynamics of primary and new production in the northern South China Sea: the significance of river discharge and nutrient advection. *Deep Sea Res. Part I Oceanogr. Res. Pap.* 53, 971–986. doi: 10.1016/j.dsr.2006.02.005
- Ley, A. C., and Mauzerall, D. C. (1982). Absolute absorption cross-sections for Photosystem II and the minimum quantum requirement for photosynthesis in *Chlorella vulgaris*. *Biochim. Biophys. Acta* 680, 95–106. doi: 10.1016/0005-2728(82)90320-6
- Li, Q., Guo, X., Zhai, W., Xu, Y., and Dai, M. (2020). Partial pressure of CO<sub>2</sub> and air-sea CO<sub>2</sub> fluxes in the South China Sea: synthesis of an 18-year dataset. *Prog. Oceanogr.* 182:102272. doi: 10.1016/j.pocean.2020.102272
- Mackey, M. D., Mackey, D. J., Higgins, H. W., and Wright, S. W. (1996). CHEMTAX – a program for estimating class abundances from chemical markers: application to HPLC measurements of phytoplankton. *Mar. Ecol. Prog. Ser.* 144, 265–283. doi: 10.3354/meps144265
- McDonald, A. E., and Vanlerberghe, G. C. (2005). Alternative oxidase and plastoquinol terminal oxidase in marine prokaryotes of the Sargasso Sea. *Gene* 349, 15–24. doi: 10.1016/j.gene.2004.12.049
- McKew, B. A., Davey, P., Finch, S. J., Hopkins, J., Lefebvre, S. C., Metodieff, M. V., et al. (2013). The trade-off between the light-harvesting and photoprotective functions of fucoxanthin-chlorophyll proteins dominates light acclimation in *Emiliania huxleyi* (clone CCMP 1516). *New Phytol.* 200, 74–85. doi: 10.1111/nph.12373
- Mella-Flores, D., Six, C., Ratin, M., Partensky, F., Boutte, C., Le Corguillé, G., et al. (2012). *Prochlorococcus* and *Synechococcus* have evolved different adaptive mechanisms to cope with light and UV stress. *Front. Microbiol.* 3:285. doi: 10.3389/fmicb.2012.00285
- Müller, P., Li, X.-P., and Niyogi, K. K. (2001). Non-photochemical quenching. A response to excess light energy. *Plant Physiol.* 125, 1558–1566. doi: 10.1104/pp.125.4.1558
- Mullineaux, C. W. (2014a). Electron transport and light-harvesting switches in cyanobacteria. *Front. Plant Sci.* 5:7. doi: 10.3389/fpls.2014.00007
- Mullineaux, C. W. (2014b). Co-existence of photosynthetic and respiratory activities in cyanobacterial thylakoid membranes. *Biochim. Biophys. Acta* 1837, 503–511. doi: 10.1016/j.bbabi.2013.11.017
- Murphy, C. D., Roodvoets, M. S., Austen, E. J., Dolan, A., Barnett, A., and Campbell, D. A. (2017). Photoinactivation of photosystem II in *Prochlorococcus* and *Synechococcus*. *PLoS One* 12:e0168991. doi: 10.1371/journal.pone.0168991
- Ni, G., Zimbalatti, G., Murphy, C. D., Barnett, A. B., Arsenault, C. M., Li, G., et al. (2017). Arctic *Micromonas* uses protein pools and non-photochemical quenching to cope with temperature restrictions on photosystem II protein turnover. *Photosynth. Res.* 131, 203–220. doi: 10.1007/s11120-016-0310-6
- Parkhill, J.-P., Maillet, G., and Cullen, J. J. (2001). Fluorescence-based maximal quantum yield for PSII as a diagnostic of nutrient stress. *J. Phycol.* 37, 517–529. doi: 10.1046/j.1529-8817.2001.037004517.x
- Pattanayak, G., and Rust, M. J. (2014). The cyanobacterial clock and metabolism. *Curr. Opin. Microbiol.* 18, 90–95. doi: 10.1016/j.mib.2014.02.010
- Paul, J. H., Kang, J. B., and Tabita, F. R. (2000). Diel patterns of regulation of *rbcL* transcription in a cyanobacterium and a Pymnesiophyte. *Mar. Biotechnol.* 2, 429–436. doi: 10.1007/s101260000016
- Pichard, S. L., Campbell, L., Kang, J. B., Tabita, F. R., and Paul, J. H. (1996). Regulation of ribulose biphosphate carboxylase gene expression in natural phytoplankton communities. I. Diel rhythms. *Mar. Ecol. Prog. Ser.* 139, 257–265. doi: 10.3354/meps139257
- Ragni, M., Aïrs, R. L., Hennige, S. J., Suggett, D. J., Warner, M. E., and Geider, R. J. (2010). PSII photoinhibition and photorepair in *Symbiodinium* (Pyrrophyta) differs between thermally tolerant and sensitive phenotypes. *Mar. Ecol. Prog. Ser.* 406, 57–70. doi: 10.3354/meps08571
- Ralph, P. J., and Gademann, R. (2005). Rapid light curves: a powerful tool to assess photosynthetic activity. *Aquat. Bot.* 82, 222–237. doi: 10.1016/j.aquabot.2005.02.006
- Raven, J. A. (2011). The cost of photoinhibition. *Physiol. Plant.* 142, 87–104. doi: 10.1111/j.1399-3054.2011.01465.x
- Raven, J. A., Beardall, J., and Quigg, A. (2020). “Light-driven oxygen consumption in the water-water cycles and photorespiration, and light stimulated mitochondrial respiration,” in *Photosynthesis in Algae: Biochemical and Physiological Mechanisms*, eds A. W. D. Larkum, A. R. Grossman, and J. A. Raven (Cham: Springer International Publishing), 161–178.
- Rocap, G., Distel, D. L., Waterbury, J. B., and Chisholm, S. W. (2002). Resolution of *Prochlorococcus* and *Synechococcus* ecotypes by using 16S-23S ribosomal DNA internal transcribed spacer sequences. *Appl. Environ. Microbiol.* 68, 1180–1191. doi: 10.1128/AEM.68.3.1180-1191.2002
- Scanlan, D. J., Ostrowski, M., Mazard, S., Dufresne, A., Garczarek, L., Hess, W. R., et al. (2009). Ecological genomics of marine picocyanobacteria. *Microbiol. Mol. Biol. Rev.* 73, 249–299. doi: 10.1128/MMBR.00035-08

- Schreiber, U., Klughammer, C., and Kolbowski, J. (2012). Assessment of wavelength-dependent parameters of photosynthetic electron transport with a new type of multi-color PAM chlorophyll fluorometer. *Photosynth. Res.* 113, 127–144. doi: 10.1007/s11120-012-9758-1
- Schuback, N., and Tortell, P. D. (2019). Diurnal regulation of photosynthetic light absorption, electron transport and carbon fixation in two contrasting oceanic environments. *Biogeosciences* 16, 1381–1399. doi: 10.5194/bg-16-1381-2019
- Schuback, N., Flecken, M., Maldonado, M. T., and Tortell, P. D. (2016). Diurnal variation in the coupling of photosynthetic electron transport and carbon fixation in iron-limited phytoplankton in the NE subarctic Pacific. *Biogeosciences* 13, 1019–1035. doi: 10.5194/bg-13-1019-2016
- Singh, T., and Bhadury, P. (2018). Distribution patterns of marine planktonic cyanobacterial assemblages in transitional marine habitats using 16S rRNA phylogeny. *Phycol. Res.* 66, 189–198. doi: 10.1111/pre.12224
- Suggett, D. J., Le Flo'c'H, E., Harris, G. N., Leonardos, N., and Geider, R. J. (2007). Different strategies of photoacclimation by two strains of *Emiliania huxleyi* (Haptophyta). *J. Phycol.* 43, 1209–1222. doi: 10.1111/j.1529-8817.2007.00406.x
- Suggett, D. J., Moore, C. M., Hickman, A. E., and Geider, R. J. (2009). Interpretation of fast repetition rate (FRR) fluorescence: signatures of phytoplankton community structure versus physiological state. *Mar. Ecol. Prog. Ser.* 376, 1–19.
- Sung, T., Yoon, S. Y., and Kim, K. C. (2015). A mathematical model of hourly solar radiation in varying weather conditions for a dynamic simulation of the solar organic Rankine cycle. *Energies* 8, 7058–7069. doi: 10.3390/en8077058
- Tikkanen, M., Mekala, N. R., and Aro, E.-M. (2014). Photosystem II photoinhibition-repair cycle protects photosystem I from irreversible damage. *Biochim. Biophys. Acta* 1837, 210–215. doi: 10.1016/j.bbabi.2013.10.001
- Tseng, C.-H., Chiang, P.-W., Lai, H.-C., Shiah, F.-K., Hsu, T.-C., Chen, Y.-L., et al. (2015). Prokaryotic assemblages and metagenomes in pelagic zones of the South China Sea. *BMC Genomics* 16:219. doi: 10.1186/s12864-015-1434-3
- Tseng, C.-M., Wong, G. T. F., Lin, I.-I., Wu, C.-R., and Liu, K.-K. (2005). A unique seasonal pattern in phytoplankton biomass in low-latitude waters in the South China Sea. *Geophys. Res. Lett.* 32:L08608. doi: 10.1029/2004gl022111
- Westberry, T., Behrenfeld, M. J., Siegel, D. A., and Boss, E. (2008). Carbon-based primary productivity modeling with vertically resolved photoacclimation. *Glob. Biogeochem. Cycles* 22:GB2024. doi: 10.1029/2007GB003078
- Wu, H., Cockshutt, A. M., McCarthy, A., and Campbell, D. A. (2011). Distinctive photosystem II photoinactivation and protein dynamics in marine diatoms. *Plant Physiol.* 156, 2184–2195. doi: 10.1104/pp.111.178772
- Wyman, M. (1999). Diel rhythms in ribulose-1,5-bisphosphate carboxylase/oxygenase and glutamine synthetase gene expression in a natural population of marine picoplanktonic cyanobacteria (*Synechococcus* spp.). *Appl. Environ. Microbiol.* 65, 3651–3659.
- Xia, X., Guo, W., and Liu, H. (2015). Dynamics of the bacterial and archaeal communities in the Northern South China Sea revealed by 454 pyrosequencing of the 16S rRNA gene. *Deep Sea Res. Part II Top. Stud. Oceanogr.* 117, 97–107. doi: 10.1016/j.dsr2.2015.05.016
- Xiao, W., Wang, L., Laws, E., Xie, Y., Chen, J., Liu, X., et al. (2018). Realized niches explain spatial gradients in seasonal abundance of phytoplankton groups in the South China Sea. *Prog. Oceanogr.* 162, 223–239. doi: 10.1016/j.pocean.2018.03.008
- Xie, Y., Laws, E. A., Yang, L., and Huang, B. (2018). Diel patterns of variable fluorescence and carbon fixation of picocyanobacteria *Prochlorococcus*-dominated phytoplankton in the South China Sea basin. *Front. Microbiol.* 9:1589. doi: 10.3389/fmicb.2018.01589
- Xu, G., Liu, J., Song, X., Tan, M., Ren, H., Li, D., et al. (2020). Diel rhythm in photosynthetic performance of phytoplankton assemblages is predicted to be light-dependent from in situ and mesocosm chlorophyll fluorescence. *J. Coast. Res.* 104, 445–454. doi: 10.2112/jcr-si104-080.1
- Zhai, W. D., Dai, M. H., Chen, B. S., Guo, X. H., Li, Q., Shang, S. L., et al. (2013). Seasonal variations of sea-air CO<sub>2</sub> fluxes in the largest tropical marginal sea (South China Sea) based on multiple-year underway measurements. *Biogeosciences* 10, 7775–7791. doi: 10.5194/bg-10-7775-2013
- Zhao, M., and Running, S. W. (2010). Drought-induced reduction in global terrestrial net primary production from 2000 through 2009. *Science* 329, 940–943. doi: 10.1126/science.1192666

**Conflict of Interest:** The authors declare that the research was conducted in the absence of any commercial or financial relationships that could be construed as a potential conflict of interest.

**Publisher's Note:** All claims expressed in this article are solely those of the authors and do not necessarily represent those of their affiliated organizations, or those of the publisher, the editors and the reviewers. Any product that may be evaluated in this article, or claim that may be made by its manufacturer, is not guaranteed or endorsed by the publisher.

Copyright © 2021 Yi, Zhang, Sun, Beardall and Gao. This is an open-access article distributed under the terms of the Creative Commons Attribution License (CC BY). The use, distribution or reproduction in other forums is permitted, provided the original author(s) and the copyright owner(s) are credited and that the original publication in this journal is cited, in accordance with accepted academic practice. No use, distribution or reproduction is permitted which does not comply with these terms.